Multibeam Micro-Drilling with High-Power Ultrashort Laser Pulses: 2-Stage Beam-Splitting Strategy and Implementation

Emeric Biver*[1], Julien Dupuy[1], Yves Hernandez[1], Anne Henrottin[2], Julien Pouysegur[3], and Roberto Ocaña[4]

[1]*Multitel Innovation Centre, Belgium*
[2]*LASEA S.A., Belgium*
[3]*AMPLITUDE, France*
[4]*Tekniker, Basque Research & Technology Alliance, Spain*
Corresponding author's e-mail: biver@multitel.be

In this paper, we describe a 2-stage laser beam-splitting strategy based on both polarization refractive and diffractive optics, and its implementation into independent modules. In the first stage, only refractive polarization optics is used and a variable number of sub-beams is produced, each sent to a different processing unit. The second stage, based on diffractive optics, splits further the sub-beams before they enter into the laser processing heads. Each resulting bundle of beamlets is then focused on the workpiece through a single focusing lens. We present the modules developed from this approach, the technical challenges involved and different practical ways to address them. One of these challenges is handling a high-power ultrashort laser radiation and hence, thermal regulation and potential damages to the system need to be considered. We discuss the implementation of the developed beam splitting units into a prototype with a kilowatt femtosecond laser, used to drill micro-holes in large Titanium metal sheets for an aeronautical application.
DOI: 10.2961/jlmn.2023.01.2007
Keywords: beam-splitting, beamlet, DOE, laser drilling, kilowatt femtosecond laser

1. Introduction

Ultra-short pulse (UPS) lasers are getting more and more powerful. This promises to open up some new possibilities in terms of machining speed. However using a too powerful beam might lead to thermal accumulation on the samples and the loss of the (thermal) advantage of having short pulses [1]. There are several solutions to this problem. One consists in optimizing the thermal impact by doing simulations to observe and limit hotspots for a given micromachining pattern [2]. Another one consists in moving the beam quicker on the workpiece, using high speed scanning technology with fast polygon mirrors [1] [3]. Another solution that receives a lot of attention is parallelization. The idea is to use multi-beam processing by splitting a single powerful laser beam into several beamlets with a spatial light modulator (SLM) [3-4] or a diffractive optical element (DOE) [1] [5-7]. For example, a technique called Diffractive Laser-Induced Texturing (DLITe) [8] has been used for the nano-structuring of superhydrophobic surfaces [9]. SLMs for beam splitting have also received interest, but so far, they have been shown to be less resistant, in spite of their high degree of flexibility [2]. More recently, research teams have been using DOEs along with acousto-optical modulators (AOMs), which is less flexible but faster and able to withstand much more power [2].

Using USP lasers with higher machining capabilities is of interest to many industrial areas. One of them is aeronautics and the high-speed micro-drilling process for Hybrid Laminar Flow Control (HLFC) panels. HLFC is a drag reduction technique used to limit turbulent flow on aircraft wings and thus decrease fuel consumption. It consists in applying suction near the leading edge of a wing, which increases laminar flow [10]. The suction is achieved through thousands of micro-holes in the range of 50 to 100 µm in diameter. The corresponding drilling process of the large HLFC panels needs to have short processing time, precise positioning of the holes and reduced thermal distortion [11]. Currently micro-drilling of large panels for HLFC is done by laser drilling, using either single pulse drilling (pulses of tens to hundreds of microseconds) or percussion drilling (pulses in the nanosecond range). Both techniques have advantages and disadvantages but both of them need post-processing to eliminate burrs. Moreover, the micro-holes must be analysed statistically to ensure that the diameters are within the required tolerances and to measure the percentage of blocked holes. Drilling with USP lasers (in the picosecond and femtosecond range) increases the hole quality and could eliminate the post-processing steps. But in the past their drilling rates have been too low for an industrial process. Using higher power USP laser with parallelization techniques could make them compatible with industrial requirements and eliminate costly and time-consuming post-processing steps.

In this paper we report on a 2-stage beam-splitting approach developed within the MULTIPOINT European project. The goal is to develop a parallel processing station using a kilowatt (kW) femtosecond laser in order to demonstrate the drilling of good quality holes with rates compatible with industry requirements. The beam-splitting strategy consists in having two stages of splitting, as illustrated in Figure 1. The first splitting stage consists in a single module based on polarizing optics. This stage provides flexibility on the number of sub-beams and allows to send these sub-beams into several scan heads, which increases

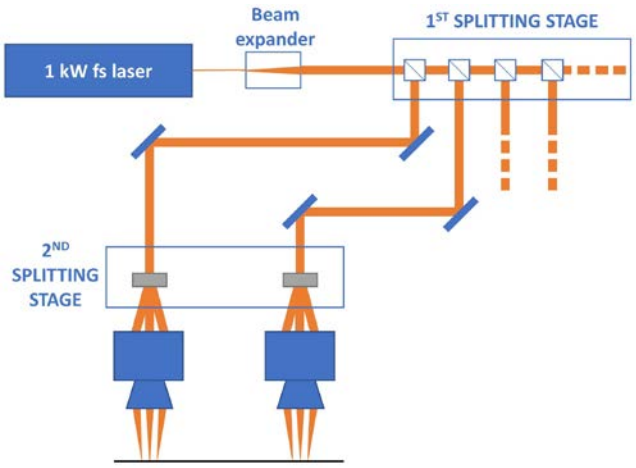

Fig. 1 Illustration of the two-stage beam-splitting strategy.

parallelization. Then the sub-beams, in the range of hundreds of watts, are sent to the second splitting stage. These modules are based on beam-splitting DOES, bulk optics that divide an incoming laser beam into several beamlets. The purpose of this stage is twofold: 1- to allow the multibeam to travel to the scan head in a controlled way (notably avoiding clipping of the beamlets), and 2- to allow a certain degree of flexibility to obtain the correct pitch between the focal point on the sample.

2. First beam-splitting stage

The module of the first stage makes use of the linear polarization of the input beam. As illustrated in Figure 2, it is composed of several sub-modules, each one composed of a half waveplate and a polarizing beam splitter (PBS) plate. The waveplate allows to turn the polarization to the desired ratio of S and P components. When the input beam comes at the optimum angle of incidence (AOI) on the PBS plate, the part of the beam that is P polarised is reflected while the part of the beam that is S polarised is transmitted. By having 4 sub-modules and a few mirrors, it is possible to have 5 exit beams and to adjust the power ratio between each output sub-beams by rotating the various half waveplates (see Figure 2).

The main technical challenge is that this module handles a very powerful laser beam. In order to reduce the power and energy density on the optics, we work with a large beam (diameter around 8 mm at $1/e^2$). This implies using large optics (2 inches in diameter in our case) to limit clipping. The module being designed for a 1 kW laser beam, for losses estimated at 5%, the module needs to dissipate 50 W. We insert a water-cooled cold-plate within the base of the module, positioned towards the entrance of the module. For most configurations, this is where the optics will handle most of the power from the input beam, and where the temperature increase due to losses is likely to be more important. The cold plate is connected to a global cooling circuit dedicated to the splitting units. The temperature inside the module is monitored by 3 thermocouples embedded within the base at 3 different locations. The module also features a water-cooled beam dump, positioned directly in front of the module input, able to absorb all the laser power if required. This design allows the tuning of the total output power from zero to maximum.

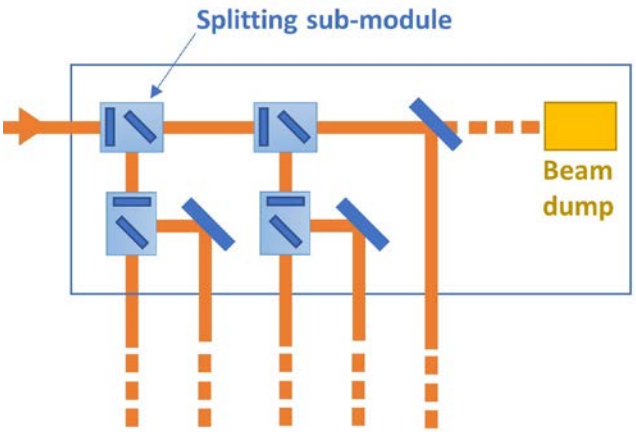

Fig. 2 Working principle of the first-stage splitting module.

The PBS plates are key elements of the module for two reasons: they are the ones doing the actual splitting, and they are also key to the alignment. This is because, in order to limit the number of mirrors and therefore the losses and the module footprint, some output beams are directly reflected from a PBS plate. We design the module so that the output beams are perpendicular to the input beam, using PBS plates designed to have a 90° optimum AOI (Angle of Incidence). To determine their actual optimum AOI, we measure their transmission and reflection extinction ratios (ratio between input power and minimum power) according to various AOIs (Figure 3).

We found that the transmission extinction ratios are almost unaffected by the AOI of the input beam (within a certain range of course). This means that the alignment of the PBS plates is not critical for the extinction of the transmitted sub-beams. The value of the transmission extinction ratio is around 1300:1. On the other hand, the reflection extinction ratios are highly impacted by the AOI, as illustrated in Figure 3. That means that when the AOI is outside the optimum range (approximately ± 1° in angular width), a fraction of the P polarised light starts being reflected instead of being all transmitted. Maximum reflection extinction ratios are around 350:1, but they decrease quickly when the AOI exits its optimum range. This means that it is critical to align the PBS plates at the centre of their

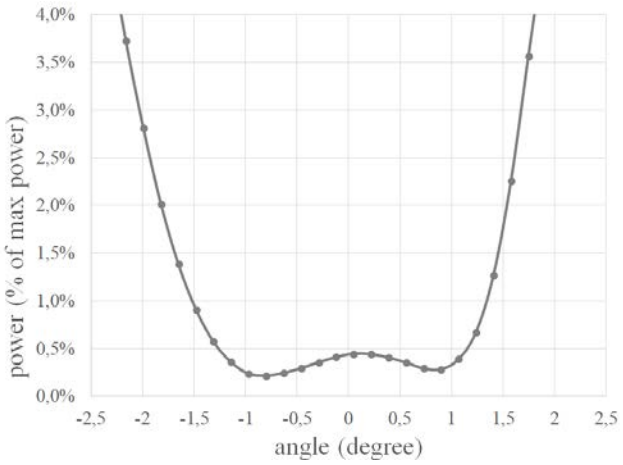

Fig. 3 Typical reflection extinction ratio for a PBS plate according to the AOI (centred on the optimum AOI).

optimum AOI range to minimise the sensitivity to beam pointing issues, and to allow the highest extinction in each arm.

We also found that the optimum AOIs are all higher than 90° by a few degrees. This optical defect poses a problem because the module is designed mechanically so that the input and output beams are perpendicular. When aligned this way, the AOIs are not optimum, which means we do not reach maximum extinction and cannot completely extinguish sub-beams. Moreover, if the AOIs are not in their optimum range, the sensitivity of the output power to a tilt of the input beam is high, as can be seen in Figure 3. For instance, a tilt of 4 mrad (0.23°) induces more than 25% standard deviation in the output power. To limit this effect, it is important to follow a specific alignment procedure to make sure that all PBS plates are aligned at the centre of their optimum AOI range. Doing so does not eliminate completely the beam pointing sensitivity (because the reflection extinction ratios are not perfectly flat within the minimum range), but significantly reduces it. The same tilt in the input beam then has less impact on the power splitting ratios (less than 2% standard deviation). This also optimises the extinction ratios and facilitates the procedure to balance the input power between the several outputs.

On the other hand, having non-perpendicular sub-beams inside the module means they are not all hitting the optics at the centre. Because the beams travel for long distances within the module (tens of centimetres), this increases the likelihood of clipping the sub-beams. We found we could minimize this issue by positioning the PBS plates with the optimum AOI closer to 90° in key positions within the module and using the few mirrors within the design to compensate for some of the non-perpendicular sub-beams. Some output beams still have a small tilt, which in our case is of no consequence due to the flexibility of the optical path after the module in the global laser micromachining system.

3. Second beam-splitting stage

Each sub-beam exiting the first stage module propagates to a dedicated carriage on a motorized stage. This is where the second splitting stage occurs. On each carriage, a module splits the incoming sub-beam into a bundle of beamlet that is then injected into the scan head and focusing lens positioned just after. This module impacts the fluence on the sample (through the beam quality and the splitting ratio into a specific number of beamlets), the pitch between the focused spots (through the angle between the beamlets) and their position. It needs to be compact, light (to limit the constraints on the motorized stage), vibration-resistant and reasonably easy to align. The following section describes the solutions we implemented to optimize these parameters.

3.1 Using laser multi-beams

Using laser multi-beams through scan heads is a technique mostly induced by the development of increasingly powerful ultra-short pulse lasers, and has been mainly addressed in the past few years [1,5]. One goal is to build a multi-beam system with accuracy over the maximum of the scanner working field using DOE technology. The beamlets bundle created by the DOE can either diverge or, through an optical relay system, converge into the scan head. Having a relay system is not absolutely necessary, but useful to mask unwanted orders (which otherwise could affect the process). A 4F system is usually used, with two focusing lenses and an intermediate focal point.

However, using such a system poses challenges. For example, there is a compromise between uniformity (of the several beamlets power) and efficiency (amount of power lost to unwanted higher-order beamlets) [6]. Also, DOEs with high numbers of beamlets and large deflecting angles introduce chromatic aberrations and the pitch between spots is no longer linear on the scan field [5]. To limit these effects, it is possible to use a smaller angle DOE with a large beam diameter, with a beam reducer (BR) before the relay system and a beam expander (BX) after it. The smaller beam diameter within the relay system increases the size of the focal spot, which makes it less likely to damage optical elements positioned inside the relay system (AOM or mask for example). It also increases the beam separation angle and limits the chromatic aberrations. Using a DOE with a non-periodic pattern or an F-sin(theta) lens allows to obtain a linear pitch on target [1].

Another challenge is the distortion of the beamlets pattern on the scan field. On a single beam regular XY scan head and focusing lens, barrel and pin-cushion distortions are usually corrected for by using a calibration file, which changes the angular positions of the scan head motors to reach a specific XY coordinate on the sample. But introducing a multi-beam instead of just a single beam creates a further problem: the correction file only compensates for the position of the centre of the multi-beam, and not for the whole multi-beam. Thus, away from the centre of the field, the multi-beam shape experiences a distortion [6].

Several solutions have been imagined to correct for or eliminate this effect. It is possible adapt the scanning system and use cylindrical lenses instead of spherical ones, to separate X and Y scans and have the beams hit the mirrors perpendicularly. This technique is efficient but very specific and requires bulky, custom optical elements [6]. A simpler approach consists in dynamically rotating the DOE to compensate for the pattern rotation on target, but some deformation remains. Another effective technique consists in compensating individually and dynamically for each beamlet. Wedges correcting the position of individual beamlets can be used [6], but this is hard to implement beyond a 2 x 2 multi-beam pattern. It is also possible to introduce an array of AOMs (acousto-optical modulators) to turn the individual beamlets ON and OFF according to their position. This works only for fast scanning and the AOMs can be damaged if the pulse energy is too high. To limit the energy density, a solution is to use a prisms array instead of 4F lenses as a relay system, to avoid internal focal points, [5]. Another simpler solution is to use passive correction, by using a low aberration focusing lens and limiting the size of the scan field where the distortions are acceptable for a given process.

3.2 Choosing the splitting method

We use DOEs for the second stage splitting because once we choose the correct splitting ratio, it can stay constant, and we are dealing with high power laser beams. By comparison, SLMs have a very high degree of flexibility

that we do not need, are more complex to use and tend to be more sensitive to the power density.

A DOE, through a micropattern etched on a functional surface, splits an incoming laser beam into several beamlets with the same characteristics (beam quality, beam diameter, divergence, etc), each with a fraction of the incoming power and each positioned at a specific angle regarding the incoming beam. An ideal DOE only splits the input beam into the desired number for sub-beams, but in practice the machining process introduces imperfections creating residual higher order beamlets carrying a small fraction of the power. Single layer patterns give a better homogeneity (on the beamlets of interest) while multi-layers patterns have higher efficiency (less power in the higher order beamlets). We use DOEs where the pattern is directly etched into the optics (fused silica) to obtain a high damage threshold.

The target hole separation for the HLFC panels is 0.5 mm, but tests have shown that drilling simultaneously holes that are that close to each other lead to significant thermal effects. We choose to implement a pitch of 1 mm, which corresponds to an angle between beamlets of 0.01 rad or 0.57 degrees for a 100 mm telecentric F-theta focusing lens

3.3 Choosing the number of beamlets

The number of beamlets depends on the process conditions, i.e. the fluence range we need to reach for drilling, and on the laser specifications on the other hand, i.e. the available power, repetition rates and beam quality. From the process perspective, we need to reach a few hundreds of kHz [12] with a fluence of a few tens of J/cm². Using the laser specifications provided by our partner Amplitude, we are able to estimate the size of the focal spot after the focusing lens and therefore the fluence for any given number of sub-beams. We show the results in Figure 4.

We want to reach a sufficient fluence at 700 kHz, the main working repetition. We try two different strategies: 1- increasing parallelization and thus having a standard maximum fluence, i.e. similar to the fluences available with standard, commercially available femtosecond lasers (usually below 15 J/cm²); 2- trying to achieve higher fluences to study the impact on the drilling process, and thus limiting the parallelization. For the first strategy, we decided to use two second-phase splitting modules, and therefore an even number of beamlets. We choose to have two 2 x 2 spots (beamlets forming a square) and therefore 8 spots total. We can thus theoretically reach 17 J/cm² at 700 kHz. For the second strategy, we use only one second-phase splitting module, with a 1D splitting (spots in a line rather than a 2D pattern) of 5 spots. The same input power being handled by a single module, fluences on optical elements increase significantly compared to the two-modules option. The specific number of spots has been chosen to limit the fluence on optical elements as well as air ionization.

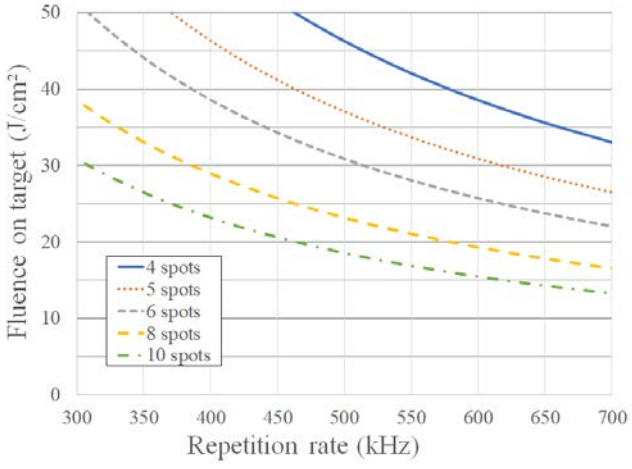

Fig. 4 Calculated fluence on the sample according to the repetition rate, for several splitting ratios.

3.4 Choosing the optical design

At the exit of a second stage module, the beamlets bundle either diverges or converges, depending on the optical design selected. If it diverges (design A), the beamlets crossing point is before the scan head. If they converge (design B), the beamlets cross inside the scan head. The position of the beamlets crossing and the overall diameter of the beamlets bundle must be optimized to ensure there is no clipping along the path, in the module, the scan head or on the focusing lens. Design A uses a beam-splitting DOE and possibly a few additional optical elements and is therefore simpler to implement than design B. But because the beamlets diverge from each other, the probability of clipping is higher. Design B uses a beam-splitting DOE and relay optics (4F system). The goal is to have the beamlets overlap between the two scanner mirrors to minimize clipping, the energy density on the mirrors and distortions introduced by the F-theta focusing lens. But as mentioned, design B increases the complexity and footprint compared to design A.

With design A, the only way to filter unwanted higher-orders would be to let the beamlets propagate on a long enough distance and use a mask when they are not superimposed anymore. Obviously, for lower angle DOE (our case), this solution is impractical in a splitting module that has to be compact. If the orders are not filtered, there will be residual spots of lower fluence on the surface of the sample during the drilling process. Design B allows to do a spatial filtering by positioning a mask close to the intermediate focal point within the 4F telescope system and letting through only the orders of interest. This means we need to be able to absorb potentially powerful laser beams close to a focal point without damaging the mask.

Also, because we have both a femtosecond laser and a high energy beam, focusing it can lead to air ionization and beam degradation if the power density is too high. For our wavelength and pulse duration, we measure the minimum power density required to ionize the air at around 5.10^{13} W/cm². The actual power density within the modules will depend on the pulse energy (which, at constant power, depends on the repetition rate and the number of sub-beams) and the focal spot size (which depends on the focal length of the telescope focusing optics, the beam diameter and the beam quality M² factor). By estimating the M² and available power for the final laser, we can simulate different configurations. For the number of spots we consider and with a beam diameter of 8 mm, the energy density gets too close to the limit. Because we need the modules to be compact, it is impractical to increase the 4F lenses focal lengths too

much, so in order to have a bigger intermediate focal point, we need to decrease the beam size and introduce a BR (beam reducer) of appropriate ratio. This means we also need to have a BX (beam expander) after the relay optics to bring back the beamlets to the original diameter of the input beam.

Compared to design B which has a BR, 4F system and a BX, design A is more compact and therefore lighter. This is important to consider as the modules will have to be positioned on moving carriages, themselves on motorized stages with a limited weight they can handle to stay within their specifications. There is also a maximum space available to fit the modules, so bigger designs require higher design efforts to keep within the space. Design B will also be harder to align, having more optical elements.

Positional and telecentricity errors both could impact the drilling process. Simulations were done, in collaboration with lens suppliers, in order to estimate the impact of the multi-beam, the position of the beamlets crossing and the position in the working field on these types of errors. One simulation was done for the telecentricity error and the Z focal position error. It was found that for a multi-beam, these two errors are similar to the errors expected with a single beam, if the distance of the DOE from the first scan mirror is below 50 mm. If this distance is increased, the errors increase as well but remain acceptable. For example, the Z error stays within the Rayleigh range (couple of hundreds of micrometres in our case). Moreover, these errors are in the same range for designs A and B: design A would introduce small errors that would be acceptable for the process compared to design B. Another simulation was done for the XY error, i.e. the horizontal positioning error on the working field. It appears that the difference of design (whether the beams cross at the level of the mirrors within the scan head or before the scan head) has almost no impact on the XY positioning errors. As seen above, calibration does not correct the multi-beam pattern distortion. Some active methods can compensate for this type of error, but they are rather heavy to implement, adding optical and electronic complexity to the module. We choose to use passive methods: using a focusing lens with the least amount of distortion possible and restraining the scan field to a smaller portion of what would be available, since the distortion is negligible at the centre and only becomes significant on the sides.

If the Telecentricity and XYZ positioning errors do not help much to discriminate between designs A and B, looking at the impact on clipping does. Design B is clearly better for this criterion, since once the beamlets bundle has entered the scan head, it gets smaller and creates an image of the beam-splitting DOE at the ideal position for the F theta telecentric lens. Design A, with its diverging bundle, increases the probability of clipping on the scanner mirrors and especially on the entrance of the focusing lens. This is especially true if the distance between the DOE and the scan head increases. Consequently, having a diverging beam forces to limit the scan field to avoid clipping exterior beamlets on the side of the lens. It also increases the distortion of these exterior beamlets, because they are closer to the periphery of the scan field.

Table 1 and Figure 5 summarise and illustrate the several design criteria and the respective advantages and drawbacks of designs A and B. We have chosen to implement design B for our modules. This is mainly based on clipping, as our beam size and divergence angle between beamlets are fixed, and, as we have seen, we want to implement 1D as well as 2D patterns for the multi-beam. The 5 spots, 1D pattern has a wider angle since the beamlets are on a line and a diverging bundle will be clipped as early as the second mirror of the scan head. The problem is less significant with the 2 x 2 2D pattern because the maximum angle is smaller. But restrictions on the scan field need to be avoided as much as possible if we are to maximize the drilling yield. Our design strategy is to select design B, compact it as much as possible from the optical point of view, and then optimize the mechanical design in order to fit within the size and weight limits of the carriages.

Table 1 Comparison between designs A and B (the best design for a given criterion is underlined)

Criteria	design A	design B	Remarks
1- Filter unwanted beamlets	NO	YES	design B: risk of ablating the mask
2- Air ionization	NO	YES	design B: reduce size of focal spot
3- Size, weight, easy to align	BEST	WORSE	design B: optimize
4- Z focal position and Telecentricity error	YES	BEST	
5- Impact on XY position	YES	YES	similar for designs A and B
6- Impact on clipping	YES	BEST	design A: also reduces the scan field

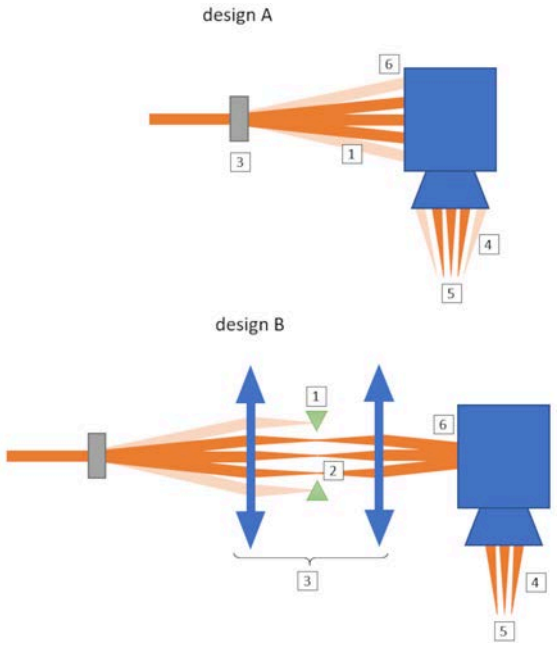

Fig. 5 Illustration of the comparison between designs A and B (numbers correspond to elements in Table 1)

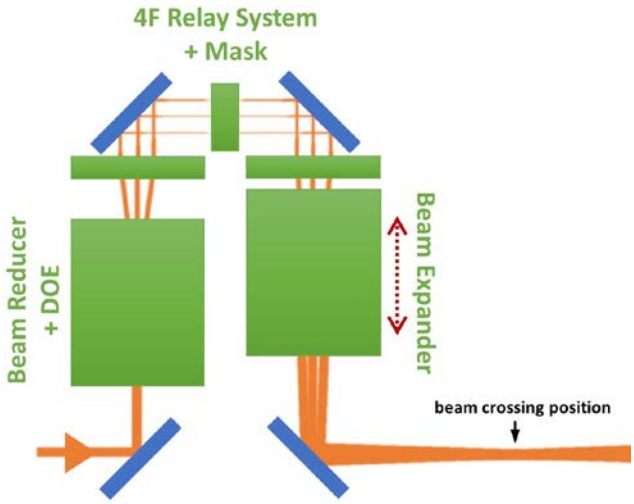

Fig. 6 Representation of the different elements of the second-phase spitting module.

As mentioned and shown in Table 1 and Figure 5, two other challenges need to be addressed with design B. Air ionization within the 4F relay system is avoided by introducing a BR and choosing appropriate focusing lenses. The possibility of ablating the mask which cuts off the higher order beamlets is addressed by using a custom water-cooled mask positioned after the focal point. The final design, shown in Figure 6 is then comprised of:

- a BR which reduces the size of the beam to avoid air ionization in the subsequent 4F system and a DOE that splits the beam;
- a 4F relay system which 1- geometrically inverts the bundle so that the beamlets converge towards each other, and 2- allows to position a mask to spatially filter the higher, unwanted orders from the DOE;
- and a BX which 1- expands the beamlets back to the same size than the original input beam and 2- controls the distance at which the beamlets cross, by adjusting its position compared to the 4F.

3.5 Opto-mechanical solutions

In parallel to the optical design, opto-mechanical solutions have to be found in order to respect the specifications. Especially, it is important to optimize the weight and footprint of the splitting modules, while ensuring that they are reasonably easy to align and use, and that no components is damaged by the high laser power and energy.

Each module is placed on a moving carriage where the input beam and the output beamlets are horizontal. Four mirrors are mounted within both standard and specifically designed mounts, that fold the beam path into two main vertical sections. The other optical elements (BR + DOE, 4F and BX) are mounted in a 60 mm cage system in these vertical sections (see Figure 6). All optics are made of fused silica and, except for the DOE, are 2 inches in diameter to accommodate for a bundle of 8 mm $1/e^2$ diameter beamlets. The cage optical mounts are custom made and have Teflon pads to decrease friction with the steel cage rods, which makes fine alignment easier. They translate along the optical axis and can be fastened in their correct aligned position. Each custom cage mount has a mechanical and thermal contact with the water-cooled cold plate that constitutes the base of the module. This cold plate, specifically designed to constitute the base of the modules, absorbs power losses and maintains a relatively stable temperature for the optical elements, thus avoiding mechanical shifts.

The first elements in the module are the BR and the DOE. In the 8 spots design, the BR and BX have a x2 ratio, whereas for the 5 spots design it is x2.5. This is because the beamlets energy is higher when there are less of them, and increasing the beam reduction allows to increase the size of the intermediate focal spot within the 4F and therefore avoid air ionization. In all modules, the BR and BX have Galilean designs, which means they use a combination of convex and concave lenses, have no intermediate focal spot and are more compact than a Keplerian design. We use relatively short focal lengths to limit the footprint and a combination of two concave lenses instead of just one to limiting aberrations. The DOE can rotate to align the pattern on the sample surface.

The 4F lenses are positioned close to the top mirrors of the two cage systems, which means that these top mirrors are “inside” the 4F. This is because the 90° mirror mounts are too bulky to be placed between the BR / BX and the 4F lenses. This means that the beamlets are partly focused when they hit the reflective surfaces of the mirrors, and care has to be taken to avoid getting close to the damage threshold. This is done by aligning the 4F lenses in a symmetrical way around the central plane of the module, so that the spots on the first and second 4F mirrors are identical in size.

The mask is placed within the 4F, between the two top mirrors. Because we are handling a very powerful beam, the beamlets absorbed by the mask are quite powerful. For example, with a 1 kW laser and a typical DOE efficiency of 80%, the mask needs to absorb around 100 W for the two-modules configuration, and 200 W for the single-module configuration. To accommodate for this, we use several strategies to design the mask. First, we place it after the focal point, to avoid the highest fluence. The further away the mask is from the focal point, the lower the fluence, but it needs to be before the beamlets start to overlap (see Figure 7). Second, we use a surface tilted at 45°, in order to decrease the fluence further. Third, we use a specific cold plate to cool down the mask and evacuate the power. Finally, we use for the mask a material with high thermal conductivity and low damage threshold. Several materials have been tested, notably few ceramics, but they are hard to machine. We select black anodized Aluminium as a good

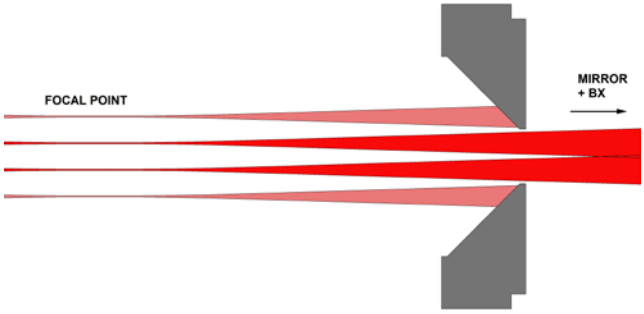

Fig. 7 Illustration of the design principles used for the shape and position of the mask.

compromise. Even if we use these design principles, we are quite close to the damage threshold fluence for the 8 spots configuration, and definitely above for the 5 spots configuration. Because of this, we choose to implement masks only in the 8 spots configuration.

The mask should be positioned very precisely in order to cut exactly the higher-order beamlets and not the main ones. This means the mechanical design needs to allow some degrees of freedom in order to align it. More precisely, the mask needs to be able to be translated 1- in the beamlets propagation axis in order to position it at the optimum position along the path (see Figure 7), and 2- in the 2 directions in the plane perpendicular to this axis, to reposition it at the centre of the multi-beam. It also needs to be rotated to fit the specific angle of the DOE, and its size needs to be adapted to the size of the beamlets bundle, which can change during the pitch tuning process. We achieve each of these degrees of freedom with a different mechanical part. The final mask design for the 8 spots configuration is compact enough to fit in the small space available between the two top mirror mounts while providing enough flexibility for mounting and alignment.

The BX is positioned in the second cage system, after the second 4F lens. During the alignment process, once the correct distance between the BX lenses is obtained, the mounts are fastened together and the BX can then be translated on the cage as a whole in order to adjust the position of the crossing of the beamlets after the module. Using a beam-viewer and some calculations, it is then possible to position this crossing position between the two scanner mirrors.

4. Implementation

This two-stages splitting strategy is designed to be implemented within a bigger drilling machine. It needs to be regulated in order to comply with the process. The two main regulations systems implemented are temperature regulation and beam pointing regulation.

Each module for the first or second phase of splitting is equipped with one or two water-cooled elements. Their purpose is to evacuate the power absorbed by the optics and the mechanical elements, and to regulate the temperature in order to limit thermal expansion and consequently beam pointing instabilities. The splitting modules have their own cooling system, with a recirculating chiller chosen so that it can provide the appropriate flow and pressure for the whole cooling circuit.

Pointing errors come from long-term thermally-induced mechanical shifts in optical mounts (notably mirror mounts), the laser (pointing instabilities), the Optical Path Compensator (device used to maintain the optical path length regardless of the carriages position on the main axis) and the motorized axis moving the scan heads over the sample (positioning errors and vibrations). A beam pointing auto-correction system is implemented for each scan head and is comprised of piezo actuated mirror mounts and 4-quadrants detectors. It allows to recover the beam deviation errors and maintain process quality over the whole sample (few meters) and overtime.

5. First results

The 5 beamlets second stage splitting module has been used in an experimental setup as illustrated in Figure 8. The kW fs laser developed in the frame of the project uses a slab amplification technology and can provide powers above 1 kW. In practice, the working power is limited to 600 W as a compromise to have a sufficient beam quality. Even so, the spot is asymmetric with different M^2 factors in the directions transversal to the propagation ($M^2x = 1.4$ and $M^2y = 1.73$), see Figure 9. The wavelength is 1030 nm, the repetition rate 700 kHz and the beam diameter ~ 3.5 mm. After the laser, a series of mirrors guide the laser beam into the splitting module and then into a galvanometric scan head designed for high power machining. The focusing lens is an asphere in fused silica of 100 mm focal length with coating for high transmission at 1030-1090 nm. The sample consists in Titanium sheets, 0.6 mm thick, in which 10 holes are drilled simultaneously using a trepanning method (jumps between two rows of 5 holes). The scan head allows the beam to oscillate in the trepanning path at a frequency of 1 kHz. The total power on the sample is 600 W and the fluence for each sub-spot is estimated at 8 J/cm².

Figure 10 shows some of the resulting holes. No burrs are observed, and microscope and X-ray tomography inspections show that the walls of the holes are straight and smooth (see Figure 11). Some oxidation can be seen on the edges of the holes. Titanium is a material that oxidizes easily when heated slightly in the presence of oxygen. Moreover, some material removed in the ablation process is redeposited on the edges of the hole. Future tests using either an

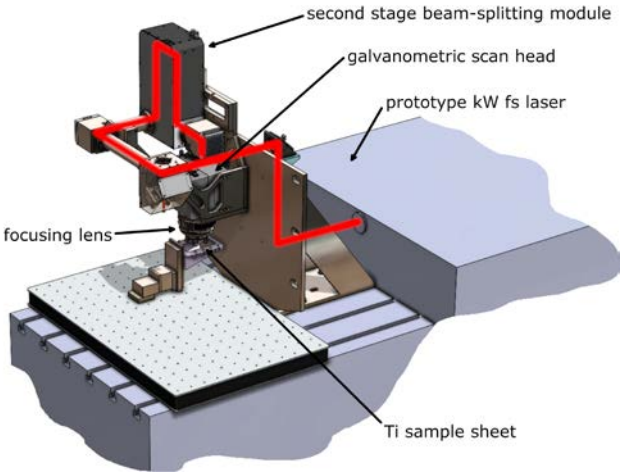

Fig. 8 Illustration of the experimental setup with the different elements.

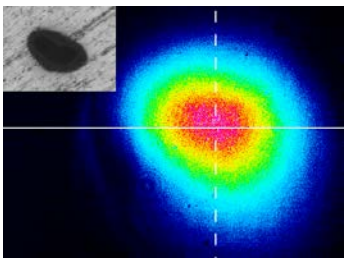

Fig. 9 . Camera image of the laser beam at the laser exit; inset: low-energy percussion ablation spot showing the shape of the focal spot on the sample.

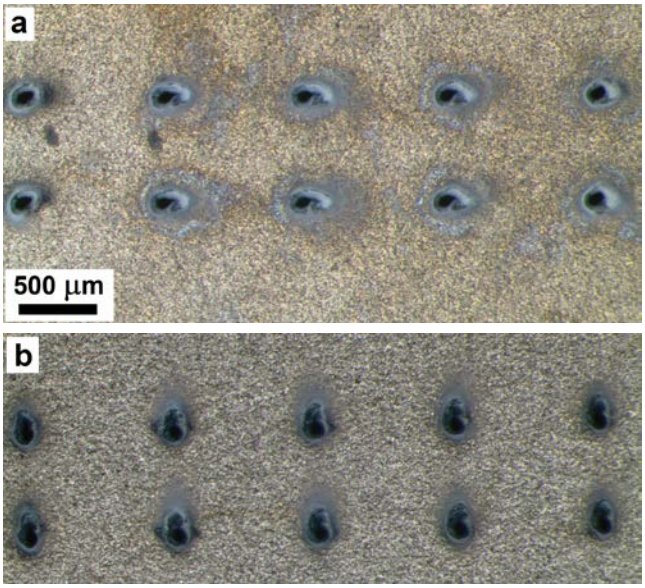

Fig. 10 Microscope images of the entrance of the holes drilled with the 5 beamlets configuration: a- 2 rows of 5 holes , b- same conditions but the DOE has been rotated by 90° as well as the image, to illustrate the fact that the asymmetrical shape is due to the laser beam.

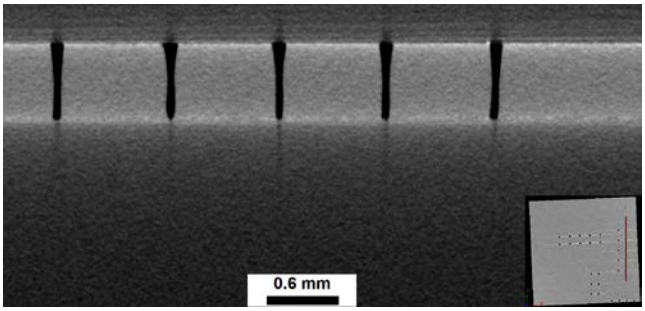

Fig. 11 . Hole profiles measured by X-ray tomography.

inert atmosphere or coaxial assist gas flow are planned to limit this effect, but here we can appreciate the extension of the zone susceptible to being affected by this phenomenon. In these tests the holes are slightly elliptical. In our opinion this is mainly due to the shape of the laser spot (see Figure 9).

These first results suggest that the combination of shape and fluence of the laser spot plays an important role in slow processes, in which ablation is the most important physical effect. Indeed, the edges of the holes are not smoothed by melting and recasting and resemble the shape of the laser spot. When the DOE is rotated 90º, the hole array is also rotated by 90º (Figure 9b). The holes made under these conditions present the same characteristics, but the asymmetry of the hole shape is preserved in space and therefore it is observed rotated 90º with respect to the direction in which the multibeam is generated. All this indicates that 1- the spot asymmetry is transferred to the shape of the hole during drilling with trepanning and 2- the main physical process is ablative without relevant contribution of thermal accumulation and melting. Regarding multibeam performance, it is observed that the novel 5-beam generator developed with custom-made diffractive optics works quite well for trepanning drilling processes based on ablation and differences between the holes drilled with different diffraction orders are small. Further steps will investigate higher fluence regimes by using smaller spots to study the material removal rate and the extent of the ablation processes versus thermal processes.

6. Conclusion and outlook

This article has presented the design and implementation of the modules in charge of the two-stage beam-splitting strategy for high-speed drilling Ti panel sheets with a fs kilowatt laser.

The fist-stage module can split the main beam into up to 5 sub-beams, each having a separate beam path after the module. The splitting is based on polarizing optics and the power of each output can be tuned individually. It has been found that the angle of the polarizing beam splitters is critical for a correct operation of the module, and special care has to be taken during alignment.

The second-stage modules are situated on carriages and positioned just before the scan heads. There are two final alternative configurations: 8 spots with 2 second-stage modules each splitting an incoming sub-beam in 4, and 5 spots with one single splitting module. The beamlets bundles then go into the scan heads and are focused on the sample as multi-spots. The splitting is based on DOEs inserted within an optical system that minimizes clipping and distortions. Several lenses within the modules allow to 1- control the fluence on the optics and avoid damage and air ionization, 2- position the crossing point of the beamlets between the X and Y mirrors of the scan head, and 3- block the unwanted residual beamlets produced by the DOE.

The modules are optimised in terms of mechanical design, compacity and weight in order to fit and be aligned on the carriages. All modules are regulated in temperature by water-cooled cold plates, and a beam-pointing correction system is implemented in order to correct for optical, thermal and mechanical instabilities. All splitting modules have been assembled and tested, and the 5 beamlets second stage splitting module has been used to successfully drill the first holes in 0.6 mm thick Titanium sheets.

The next steps are the final integration in a prototype with X,Y,Z travel stages, to drill large Ti panels using both splitting approaches (8 or 5 beamlets). This will allow to optimize the parameters and drilling yields as well to determine the performance of the technology compared to current laser drilling processes based on larger pulses and hence thermal processes for the material removal.

Acknowledgments

This work was funded by the European Union's Horizon 2020 research and innovation program under Grant Agreement nº 825567

References

[1] A. Gillner, J. Finger, P. Gretzki, M. Niessen, T. Bartels, and M. Reininghaus, J. Laser Micro Nanoeng., 14, (2019) 129.

[2] J. Finger, B. Bornschlegel, M. Reininghaus, A. Dohrn, M. Niessen, A. Gillner, and R. Poprawe, Adv. Opt. Technol., 7, (2018) 145.

[3] A. Gillner, M. Jüngst, and P. Gretzki, Proc. LiM 2015, (2015) AF3A.5.

[4] Z. Kuang, D. Liu, W. Perrie, S. Edwardson, M. Sharp, E. Fearon, G. Dearden, and K. Watkins, Appl. Surf. Sci., 255, (2009) 6582.
[5] J. Finger and M. Hesker, J. Physics. Photonics, 3, (2021) 021004.
[6] O. Hofmann, J. Stollenwerk, and P. Loosen, J. Laser Appl., 32, (2020) 012005.
[7] S. Bruening, A. Gillner, and K. Du, Adv. Opt. Technol., 10, (2021) 315.
[8] A. Brodsky and N. Kaplan, J. Laser Appl., 32, (2020) 032011.
[9] P. Hauschwitz, R. Bičštová, A. Brodsky, N. Kaplan, M. Cimrman, J. Huynh, J. Brajer, D. Rostohar, J. Kopeček, and M. Smrž, Nanomater, 11, (2021) 1987.
[10] A. Abbas, J. de Vicente, and E. Valero, Aerosp Sci Technol, 28, (2013) 100.
[11] R. Ocaña, C. Soriano, J. Esmoris, and R. Sánchez, J. Laser Micro Nanoeng.,.14, (2019) 54.
[12] D. Haasler and J. Finger, J. Laser Appl., 31, (2019) 022201.

(Received: June 24, 2022, Accepted: March 21, 2023)